STATISTICAL CONSTRAINTS ON STATION CLOCK PARAMETERS IN THE NRCAN PPP ESTIMATION PROCESS

Giancarlo Cerretto, Patrizia Tavella
Istituto Nazionale di Ricerca Metrologica (INRiM)
Strada delle Cacce 91 – 10135 – Torino, Italy
g.cerretto@inrim.it
p.tavella@inrim.it

François Lahaye
Geodetic Survey Division, Natural Resources Canada (NRCan)
Ottawa, Canada
Francois.Lahaye@nrcan-rncan.gc.ca

Abstract

In recent years, many national timing laboratories have collocated geodetic Global Positioning System receivers together with their traditional GPS/GLONASS Common View receivers and Two-Way Satellite Time and Frequency Transfer equipment. Many of these geodetic receivers operate continuously within the International GNSS Service (IGS), and their data are regularly processed by IGS Analysis Centers. From its global network of over 350 stations and its Analysis Centers, the IGS generates precise combined GPS ephemerides and station and satellite clock time series referred to the IGS Time Scale. A processing method called Precise Point Positioning (PPP) is in use in the geodetic community, allowing precise recovery of GPS antenna position, clock phase, and atmospheric delays by taking advantage of these IGS precise products. Previous assessments, carried out at INRiM (formerly IEN) with a PPP implementation developed at NRCan, showed that PPP clock solutions have better stability over the short/medium term than GPS CV and GPS P3 methods and significantly reduce the day boundary discontinuities when used in multi-day continuous processing, allowing time-limited, campaign-style time transfer experiments. This paper reports on follow-on work performed at INRiM and NRCan to further investigate the effects of applying statistical constraints on station clock parameters in the PPP estimation process, specifically its impact on short-term noise of the clock solutions and recovery after receiver loss of lock on incoming signals.

INTRODUCTION

Time and frequency transfer using GPS code and carrier phase is an important research activity for many institutions involved in time applications **[1,2]**. This was recognized when the International GNSS Service (IGS) and Bureau International des Poids et Mesures (BIPM) formed a joint pilot study **[3]** to analyze the IGS Analysis Centers clock solutions and recommend new means of combining them. That

study resulted in the formation of the Final and Rapid IGS time scales **[4]** as respective time references for the Final and Rapid IGS combined clock products (both stations and satellites) produced since the autumn of 2000 **[5]**.

Whereas all IGS clock solutions are network-based, software and algorithms are available to use these network-based products to process data from single stations. This offers a cost-effective way to integrate further solutions into global solutions, be it earth stations positions, clocks, or local atmospheric parameters. This paper reports on follow-on work jointly performed at Istituto Nazionale di Ricerca Metrologica (INRiM) and Natural Resources Canada (NRCan) to assess the time transfer potential of Precise Point Positioning (PPP) **[6]**.

PPP is a single station postprocessing methodology for recovering coordinates of GPS reception antennas, GPS receiver clock offsets, and local tropospheric parameters. It has been shown that PPP clock solutions are consistent with the IGS Final clock products at the sub-nanosecond level **[7,8]** and are also consistent at the 2-ns level with other relative measurement techniques, e.g., Two-Way Satellite Time and Frequency Transfer (TWSTFT), GPS Common View (CV), and GPS P3 **[9]**. Finally, PPP shows a 2-times improvement in stability over GPS CV and GPS P3, providing a frequency stability (in terms of Allan deviation) of 1×10^{-14} at 1 day **[7]**.

Taking advantage of continuous PPP solutions analyzed in **[10],** a method called Sliding batch procedure has been developed, in order to improve the continuity of solutions by minimizing the solution boundary discontinuities caused by colored-noise in pseudoranges **[11]**, through averaging over multi-day intervals of different durations **[12]**.

The main objective of this work is to assess the effects of constraining the station clock in the PPP estimation process. This means considering the previous clock state estimate as initial value for the next one, accounting for *a priori* estimated clock behavior with a model defined by a frequency offset, a frequency drift, and process noise. The objective of this procedure is to evaluate if the short-term frequency stability can be improved.

The following sections provide background information on NRCan's implementation of the PPP algorithm, the characterization of an atomic clock, and the NRCan PPP clock solution computations and analysis that have been performed in order to evaluate the issue addressed in the present work.

NRCAN'S ALGORITHM

NRCan's implementation of the PPP method was originally developed as a geodetic tool to provide single station-positioning capability within geodetic reference frames. The PPP method is a postprocessing approach using undifferenced GPS observations, coming from a single geodetic receiver along with satellite orbits and clocks products, and optionally modeled ionospheric delays for single-frequency receivers.

The parameters estimated by PPP are station positions (in static or kinematic mode), station clock states, local troposphere zenith delays, and carrier-phase ambiguities. The best position solution accuracies, reaching the few centimeters in horizontal coordinates and less than 10 cm in vertical coordinates (RMS), are obtained by processing GPS dual-frequency pseudorange and carrier-phase observations with IGS precise satellite orbit and clock products. NRCan PPP can achieve this accuracy using accurate models for all the physical phenomena involved. Further details on the PPP algorithms, models, and specifications can be found in **[6]**.

CHARACTERIZATION OF ATOMIC CLOCKS

An atomic clock is a device that provides as output an electric signal. In order to characterize its behavior, it is necessary to define a mathematical model which is able to describe the signal in all its components.

A conventionally accepted model expresses the instantaneous voltage in output of an atomic clock as **[14]**:

$$V(t) = [V_0 + \varepsilon(t)]\sin[2\pi\nu_0 t + \phi(t)] \qquad (1.1)$$

where V_0 and ν_0 are respectively the nominal amplitude and frequency of the signal, while $\varepsilon(t)$ and $\phi(t)$ are the random fluctuations of the amplitude and the phase. However, this is a simple model since in many atomic clocks, stochastic and non-stochastic perturbations are mixed and, thus, may be difficult to identify and separate.

The *instantaneous frequency* of a clock is defined as:

$$\nu(t) = \nu_0 + \frac{1}{2\pi}\frac{d}{dt}\phi(t) \qquad (1.2)$$

where $\frac{1}{2\pi}\frac{d}{dt}\phi(t)$ is the instantaneous fluctuation of frequency. In most practical applications, in order to evaluate the performance of a clock, it is convenient to compare it with respect to a more accurate and stable reference.

For this purpose, some quantities used by most metrological institutions are defined as:

- The *normalized phase deviation,* expressed as:

$$x(t) = \frac{\phi(t)}{2\pi\nu_0} \qquad (1.3)$$

- The *normalized frequency deviation*, defined as:

$$y(t) = \frac{\nu(t) - \nu_0}{\nu_0} = \frac{1}{2\pi\nu_0}\frac{d}{dt}\phi(t) \qquad (1.4)$$

Dimensionally, the *x(t)* is a time that represents the time offset between the examined clock signal and the reference one, and the *y(t)* is dimensionless and can be defined as the difference between the frequency of the examined clock with respect to that of the reference.

Following previous equations (1.3) and (1.4), $x(t)$ and $y(t)$ are linked by the following relation:

$$y(t) = \frac{d}{dt}x(t) \qquad (1.5)$$

The *Normalized frequency deviation* $y(t)$ can be reformulated assuming a linear variation:

$$y(t) = y(t_0) + d \cdot (t - t_0) + \varepsilon(t) \qquad (1.6)$$

where:

- $y(t_0)$ represents the *frequency offset* at the instant t_0;
- d represents a constant *linear frequency drift*;
- $\varepsilon(t)$ represents a generic random process in frequency deviation.

In a similar way, it is also possible to redefine the *normalized phase deviation* $x(t)$ as:

$$x(t) = x(t_0) + y(t_0) \cdot (t - t_0) + \frac{1}{2} d \cdot (t - t_0)^2 + \psi(t) \qquad (1.7)$$

where:

- $x(t_0)$ represents the *phase offset* at the instant t_0;
- $y(t_0)$ and d are respectively linear and quadratic in phase;
- $\psi(t)$ represents a generic random process in phase deviation.

The *linear frequency drift d* can be considered the main deterministic perturbation: it is a systematic frequency change in function of time, essentially due to modifications within the internal structure of the atomic clock and usually manifests itself as a constant increase or decrease of the clock's frequency. It is a systematic effect, because it recurs constantly during the measure, so it cannot be eliminated by averaging of repeated measurements **[1]**.

In addition to deterministic components, there are also random fluctuations, noises, which influence the frequency stability of a clock. For their proper identification, it is necessary to remove any deterministic components from the clock signal. Noises can be of different types and their presence and level may vary depending on the type of atomic clock. The most common noises present in precise atomic clocks are white noise on phase, flicker noise on phase, white noise on frequency, flicker noise on frequency, and random walk on frequency **[13]**.

Through appropriate statistical methods applied on phase or frequency deviation data obtained from measurements in function of time, it is possible to estimate the type and level of the dominant noise affecting the signal of an atomic frequency standard. This type of approach is called analysis in the *time domain* **[15]**. When data are considered statistically independent and randomly distributed according to a Gaussian law, it is possible to estimate their mean and dispersion, i.e. their variance, using classical statistical estimators. However, a Gaussian distribution is not always the most suitable assumption. In the presence of certain types of noise, the classical variance estimator diverges and this can depend on the number of available data.

Since sometimes it is difficult to dispose of a big number of samples, David W. Allan proposed using the smallest possible number of samples (two) to estimate many single variances and then calculate their mean to obtain a good estimation of the variance of the frequency measurements in the selected period. This procedure is known as the *Allan variance* **[15]** and it is the adopted method to estimate the frequency stability and identify the types of noise which are dominant in the clock signals.

STATION CLOCK CONSTRAINTS

For the purpose of analysis reported in the present work, the NRCan PPP software was modified to account for the noise characteristics of the reference frequency standards (i.e., atomic clocks, such as cesiums or hydrogen masers), as well as for the frequency offset and the linear frequency drift, in order to help in the receiver clock estimation process. Specifically, the user can specify constant values for station clock process noise *adev(1s)*, frequency offset *y*, and linear drift *d*. These will be used to compute the *a-priori* epoch clock state from previous states and its *a-priori* weight, dependent on the time interval:

$$\begin{aligned} y(t_K) &= y(t_{K-1}) + d \cdot (t_K - t_{K-1}) \\ x(t_K) &= \hat{x}(t_{K-1}) + y(t_K) \cdot (t_K - t_{K-1}) \\ \varepsilon(t_K) &\approx N(0, adev(1s) \cdot (t_K - t_{K-1})^{1/2}) \end{aligned} \qquad (1.8)$$

where:

- $x(t_k)$ represents the clock a priori estimate at the instant t_K;
- $\hat{x}(t_{K-1})$ represents the clock estimate at the instant t_{K-1};
- $y(t_K)$ represents the deterministic *frequency offset* at the instant t_K;
- $y(t_0)$ and d represent the user-specified initial *frequency offset* and *linear frequency drift*, respectively;
- $\varepsilon(t)$ represents a random process based on user-specified *adev*(1s).

The implemented noise model is only suitable for frequency standards affected by white frequency noise.

STATION SELECTION

For the evaluation of the station clock constraint model, some IGS stations operated by national timing laboratories have been selected, using the following criteria:

- Laboratories hosting a GPS receivers connected to an external atomic oscillator (H-maser and cesium);
- Availability of a large quantity of high-quality data (GPS observations).

A dataset of dual-frequency GPS pseudorange and carrier-phase observations, collected during the period running from 29 April 2008 (MJD 54585) to 8 May 2008 (MJD 54594), was assembled from the daily RINEX files at 30-second sampling available at the IGS data centers. The selected stations and related equipment are listed in Table I.

Table 1. IGS stations involved in the comparison.

TAI Laboratory	Country	IGS Station	Receiver	External Frequency	Time Transfer Technique(s)
USNO	**USA**	**usn3**	**ASHTECH Z-12T**	**H-maser**	**TW, P3**
PTB	**Germany**	**ptbb**	**ASHTECH Z-12T**	**Cs**	**TW, P3**
OP	**France**	**opmt**	**ASHTECH Z-12T**	**H-maser**	**TW, P3**
INRIM	**Italy**	**ieng**	**ASHTECH Z-12T**	**H-maser**	**TW, P3**
ORB	**Belgium**	**brus**	**ASHTECH Z-12T**	**H-maser**	**P3**

PPP PROCESSING OPTIONS

All PPP processing was performed using NRCan PPP Release 1087 modified as described earlier, with IGS Final 15-minute satellite orbit and 5-minute satellite clock products.

The stations position were estimated in static mode (i.e. one constant position per continuous processing period) with epoch station clock and local tropospheric zenith delay at 5-minute intervals, synchronized with the satellite precise clock epochs. The tropospheric zenith delays were estimated with a process noise of 5 mm/hour$^{1/2}$.

The receiver clock deterministic parameters input to the PPP for the "constrained" process have been computed by means of iNRiM statistical tools on the estimates provided by a previous unconstrained PPP solution for selected stations and period, with respect to the IGS Rapid products realizing the IGS Time Scale (IGRT).

Stochastic process parameter has been defined through *adev(1s)* provided by the frequency standard manufacturer.

PROCESSING RESULTS

In order to assess the constraint capabilities of the PPP, for selected stations, time and frequency analysis has been performed, organized in "cases" as follows:

- H-Maser vs. IGS Time Scale ("ieng" vs. IGRT);
- H-Maser vs. H-Maser ("ieng" vs. "usn3");
- H-Maser vs. H-Maser ("brus" vs "usn3");
- Cesium vs. IGS Time Scale ("ptbb" vs IGRT).

Additionally, two specifics "cases" have been addressed, namely:

- Intentional induced HW jumps;
- Noisy receivers.

H-MASER VS. IGS TIME SCALE ("IENG" VS. IGRT)

For the first analyzed case, the IGS permanent station operated at iNRiM and equipped with an Ashtech ZXII-3T dual-frequency receiver is considered. Timing reference for such a station is the Italian realization of UTC, namely UTC (IT), generated by an active hydrogen maser (AHM).

In the following, comparison results are presented in terms of phase offsets (Figure 1) and frequency stability, as gotten by means of the Overlapping Allan deviation (Figure 2).

In particular, in Figure 1, unconstrained and constrained solutions are presented, together with their differences.

The observed daily periodicity is mainly due to the thermal variations of the iNRiM laboratory hosting the auxiliary output generator (AOG) used for the generation of UTC (IT). The phase offset between unconstrained and constrained solutions and their slight divergence (250 ps over 10 days) is an issue still under investigation, but could be most likely due to an incorrect estimation of the deterministic parameters characterizing baseline estimates.

In Figure 2, the frequency stability in terms of Overlapping ADEV is presented for both unconstrained and constrained solutions, together with the stability of the iNRiM H-maser used as timing reference for the "ieng" Ashtech ZXII-3T receiver and evaluated with respect to an iNRiM primary standard, a Cs fountain.

From Figure 2, the short-term frequency stability is clearly improved, without masking the medium-long term estimates characteristics, in this case represented by the daily periodic signal depicted through the clearly visible "bump" in the ADEV plot.

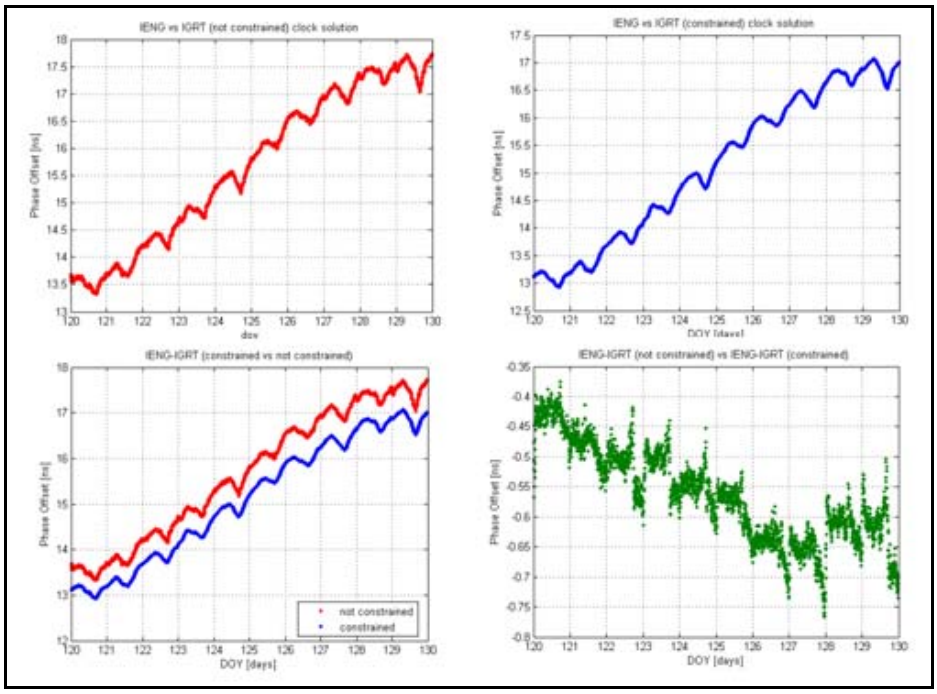

Figure 1. PPP unconstrained (red) and constrained (blue) solutions and their differences (green).

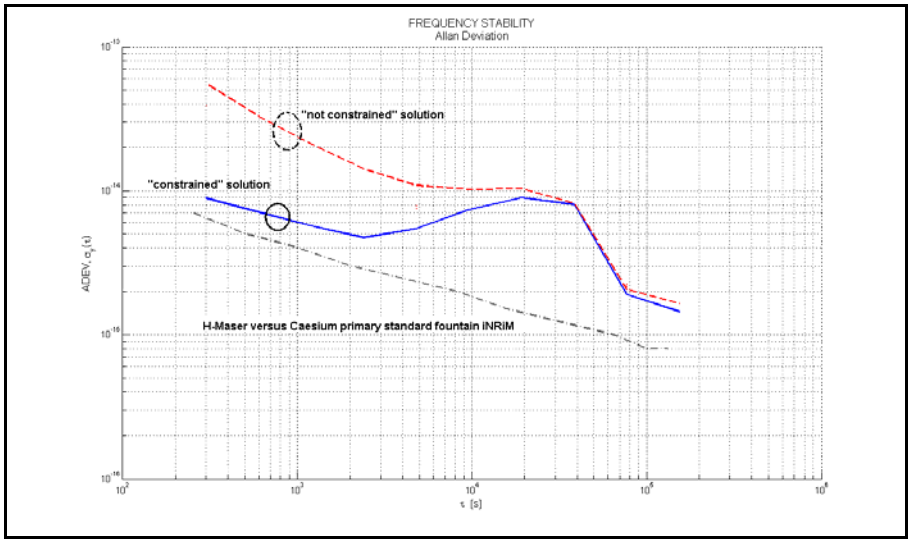

Figure 2. PPP unconstrained (red-dotted) and constrained (blue) solutions comparison in terms of frequency stability.

H-MASER VS. H-MASER ("IENG" VS. "USN3")

The "ieng" vs. "usn3" baseline, analyzed in this section, is between the iNRiM and USNO IGS permanent stations. Both stations are equipped with Ashtech ZXII-3T receivers and have as timing reference the Italian and American local realization of UTC, namely UTC (IT) and UTC (USNO), respectively.

In Figure 3, the PPP estimates are presented in terms of phase offset for both unconstrained and constrained solutions, together with the collocated Two-Way Satellite Time and Frequency Technique (TWSTFT) estimates for the same baseline. The TWSTFT estimates are available every 2 hours (7200 s), as obtained by the regular operation schedule, and for plotting purposes, a 53-ns offset has been added.

The observed daily periodicity is due to the thermal variations described in the previous section, while the divergence between both PPP solutions and TWSTFT estimates is due to the different thermal gradients affecting the GPS and TWSTFT equipment located in the two different laboratories at iNRiM.

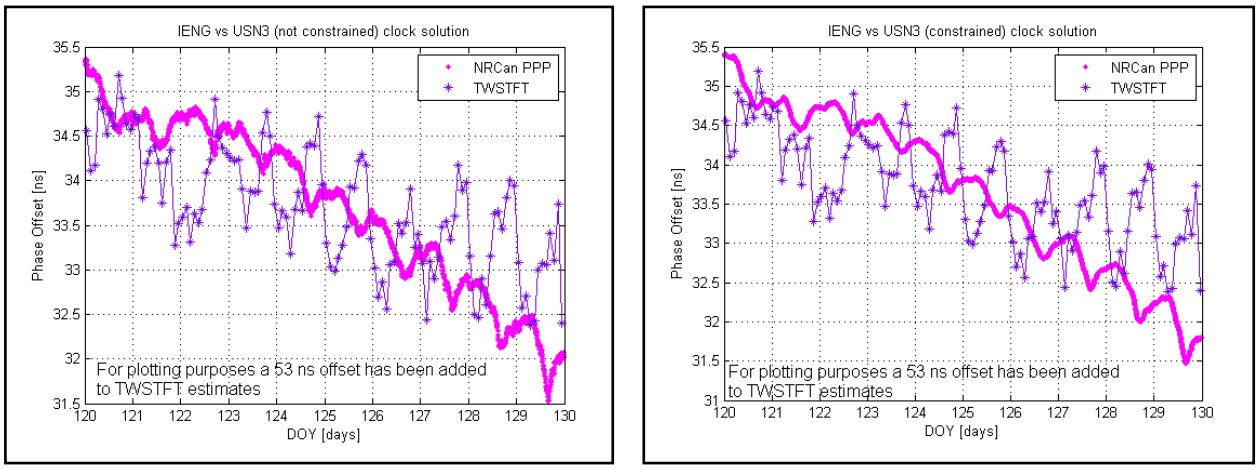

Figure 3. PPP unconstrained (pink-left), constrained (pink-right), and TWSTFT estimates (blue) comparison.

Figure 5 shows the frequency stability in terms of Overlapping ADEV for both unconstrained and constrained solutions, the TWSTFT estimates, together with the stability of the iNRiM H-maser used as timing reference for the "ieng" Ashtech ZXII-3T receiver and evaluated with respect to the iNRiM primary standard fountain.

Also, for this baseline, the short-term frequency stability is improved, without masking the medium-long term estimates characteristics, also in this case represented by the daily periodic signal depicted through the clearly visible "bump" in the ADEV plot (coming from iNRiM estimates for both techniques).

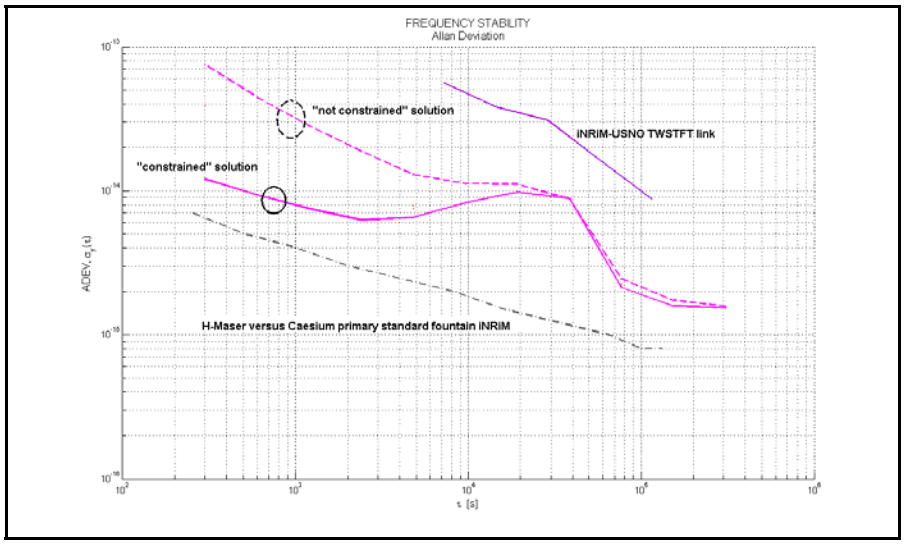

Figure 4. PPP unconstrained (pink-dotted), constrained (pink), and TWSTFT estimates (blue) comparison in terms of frequency stability.

H-MASER VS. H-MASER ("BRUS" VS. "USN3")

Another intercontinental baseline is analyzed in this section, made up of "brus" and "usn3" IGS permanent stations, both equipped with Ashtech ZXII-3T receivers and using active hydrogen masers as timing references.

In Figure 5, PPP estimates are presented in terms of phase offset for both unconstrained and constrained solutions.

Conversely to what described for the previous "ieng" vs. "usn3" baseline, no thermal periodicities are here observed.

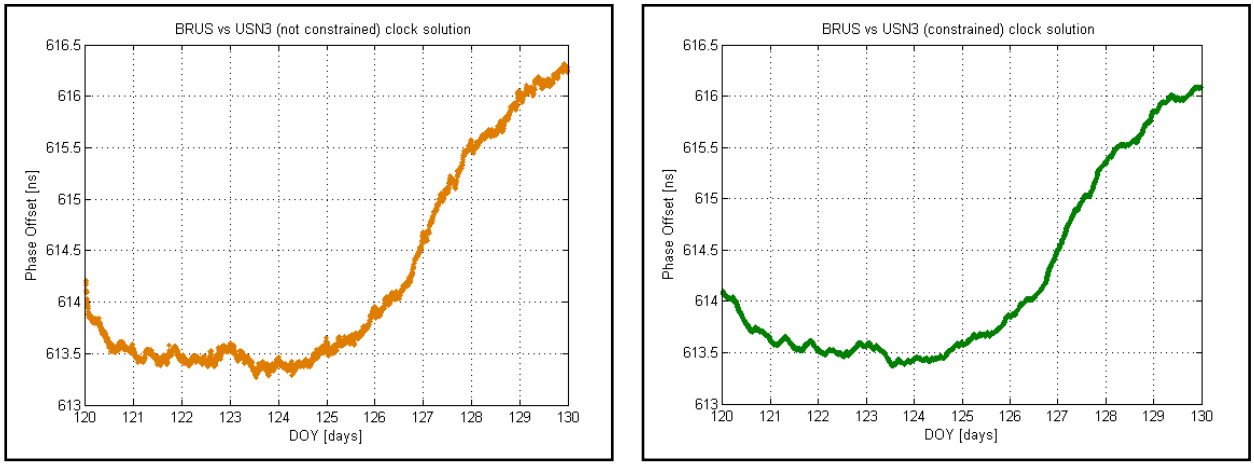

Figure 5. PPP unconstrained (brown-left) and constrained (green-right) solutions comparison.

In Figure 6, the frequency stability in terms of Overlapping ADEV is presented for both unconstrained and constrained solutions, together with the stability of the iNRiM H-maser as evaluated with respect to the iNRiM primary standard fountain. For the "usn3" station at USNO, the same H-maser frequency standard is used, while for the "brus" station a CH1-75 model is involved.

Also, for this baseline, the short-term frequency stability is improved, without masking the medium-long-term estimates characteristics.

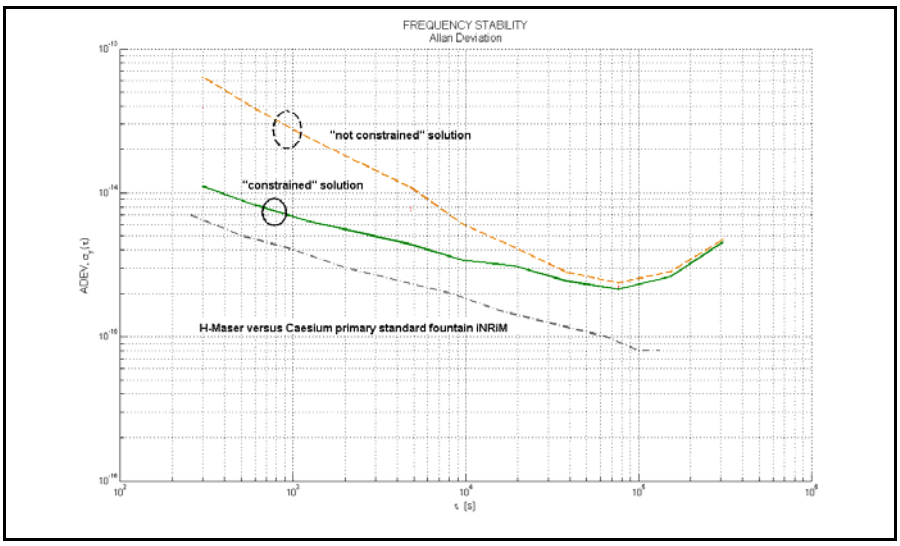

Figure 6. PPP unconstrained (brown-dotted) and constrained (green) solution comparison in terms of frequency stability.

CESIUM VS. IGS TIME SCALE ("PTBB" VS. IGRT)

Here, the IGS permanent station operated at PTB and made up by an Ashtech ZXII-3T dual frequency receiver, synchronized by the PTB Cs2 cesium primary frequency standard, is analyzed.

In Figure 7, PPP estimates are presented in terms of phase offset for both unconstrained and constrained solutions.

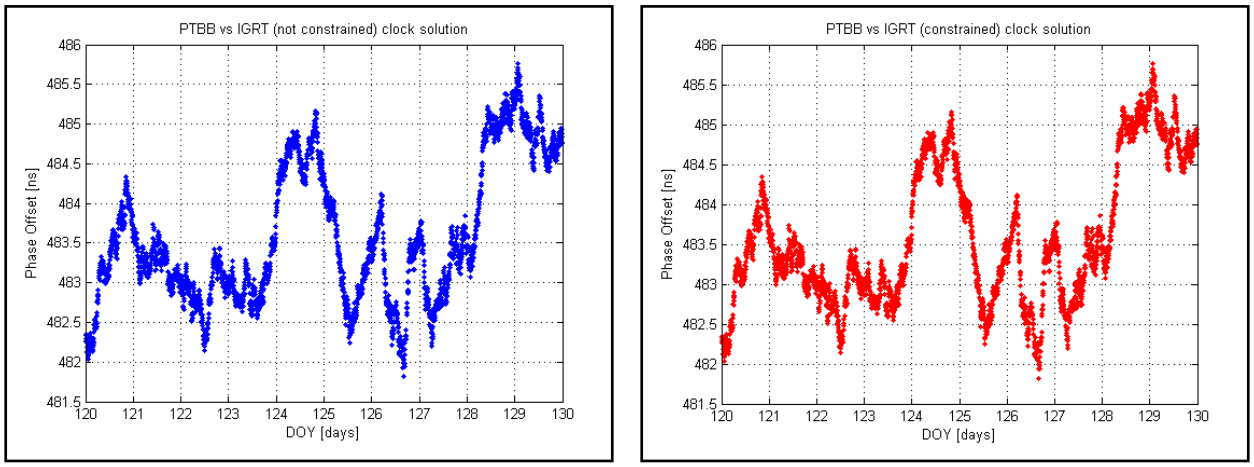

Figure 7. PPP unconstrained (blue-left) and constrained (red-right) solutions comparison.

In Figure 8, the frequency stability in terms of Overlapping ADEV is presented for both unconstrained and constrained solutions, together with the stability of the iNRiM H-maser as evaluated with respect to the iNRiM primary standard fountain and the PTB CS2 cesium primary standard used as timing reference for the "ptbb" station.

Because the Cs frequency noise dominates the PPP time transfer noise, there is no improvement in constraining PPP estimates at the level appropriate for a Cs FS.

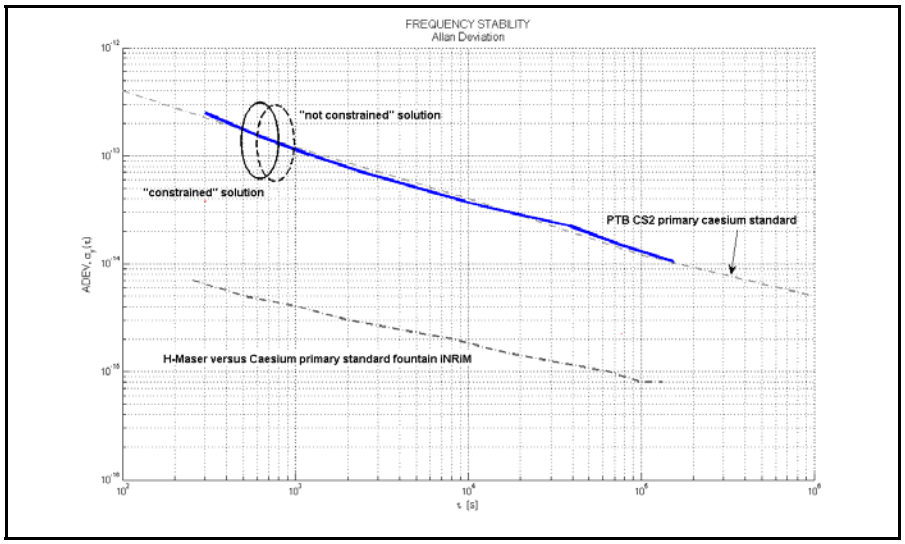

Figure 8. PPP unconstrained (blue-dotted) and constrained (red) solutions comparison in terms of frequency stability.

SUMMARY

In this section, a comparison for all stations taken into account in the present work is performed, with respect to the "rapid" realization of IGS Time Scale and in terms of phase offsets and frequency stability, as shown in Figure 9 and Figure 10.

From Figure 10 especially, a consistent improvement in the short-term frequency stability when PPP clock estimation process is achieved accounting for the deterministic and stochastic components of active hydrogen masers. For clocks with inherent higher noise dominating that of the transfer technique, adding constraints to the PPP estimation process is not required.

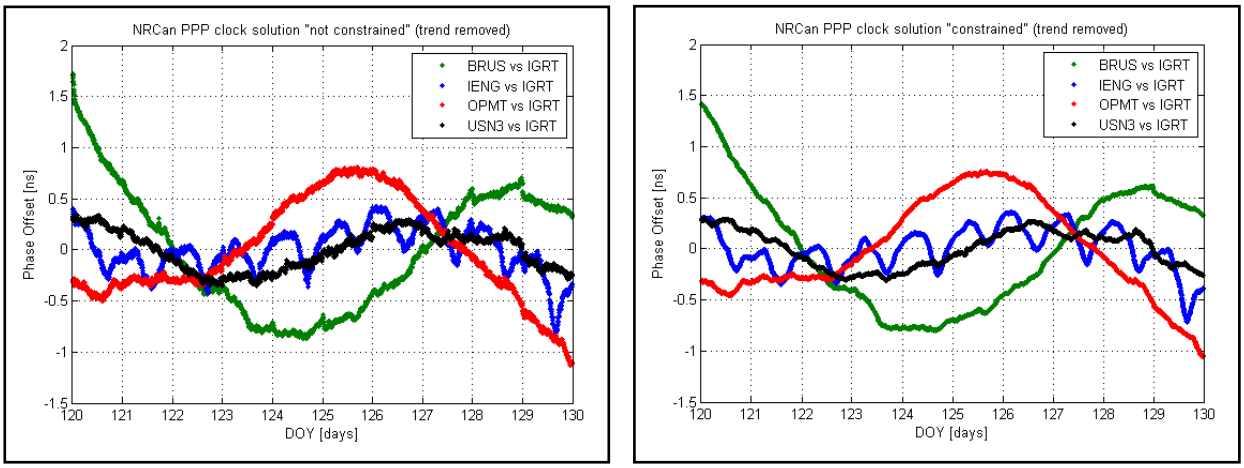

Figure 9. PPP unconstrained (left) and constrained (right) solutions for all selected stations with respect to the "rapid" realization of IGS Time Scale.

INTENTIONAL INDUCED HW JUMPS

In this section, the PPP "constrained" capabilities are evaluated in detecting intentional induced hardware jumps.

In particular, estimates related to an iNRiM geodetic receiver after having changed its receiving antenna are evaluated. 1-ns level jumps detection by means of the "constrained" PPP, in order to understand if "constraining" operation could lead to a "misdetection" of external induced jumps, is addressed.

Figure 11 shows the phase offset obtained from both unconstrained and constrained solutions.

As clearly depicted, the 1-ns level jump induced by changing receiving antenna is correctly estimated by the constrained PPP solution.

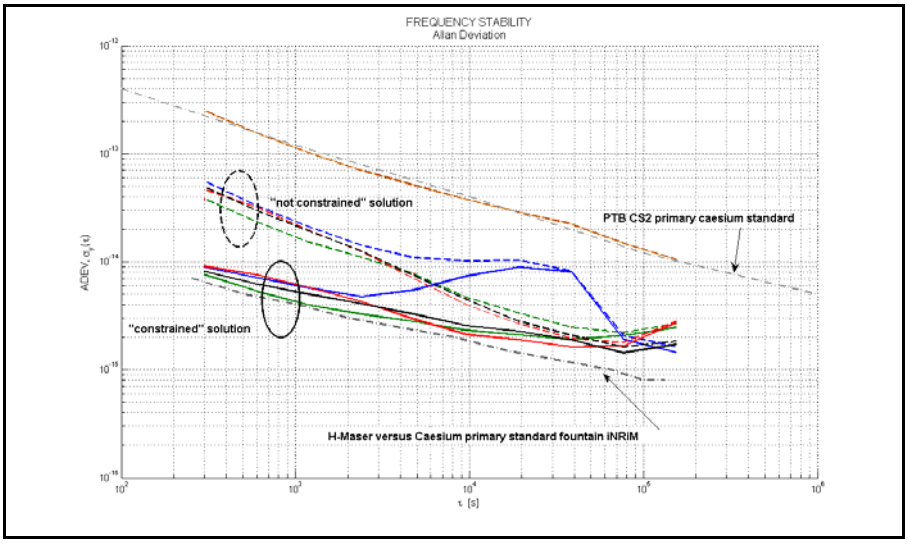

Figure 10. PPP unconstrained (dotted) and constrained solutions for all selected stations with respect to the "rapid" realization of IGS Time Scale in terms of frequency stability.

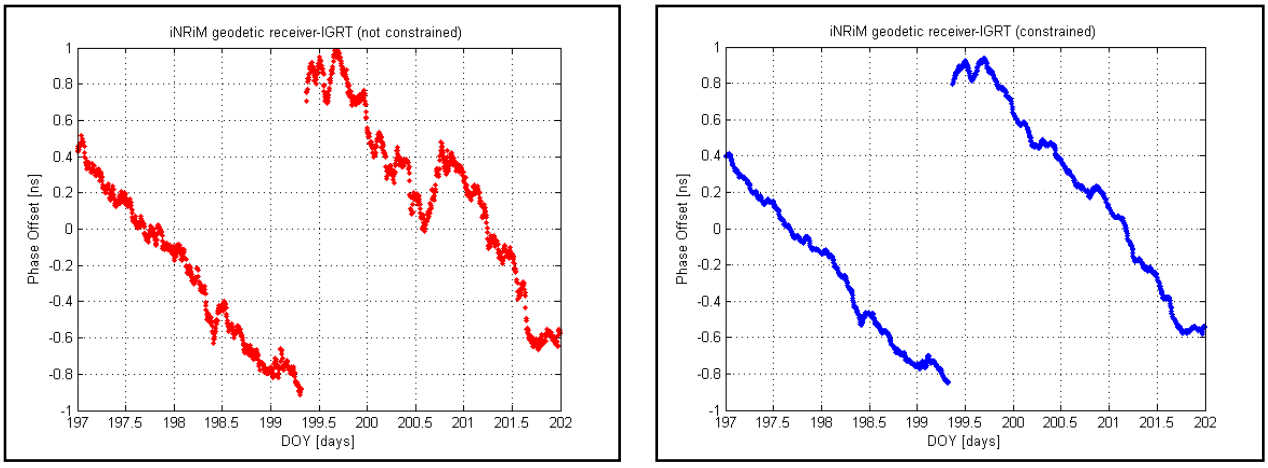

Figure 11. PPP unconstrained (red-left) and constrained (blue-right) solutions comparison for an intentional induced HW jump case.

Figure 12 shows the frequency stability computed using estimates after the antenna change and phase jump for the period after 2008 DOY 199.5.

Also, in this case, as showed in the previous sections, the short-term frequency stability is clearly improved, constraining the PPP clock estimation process.

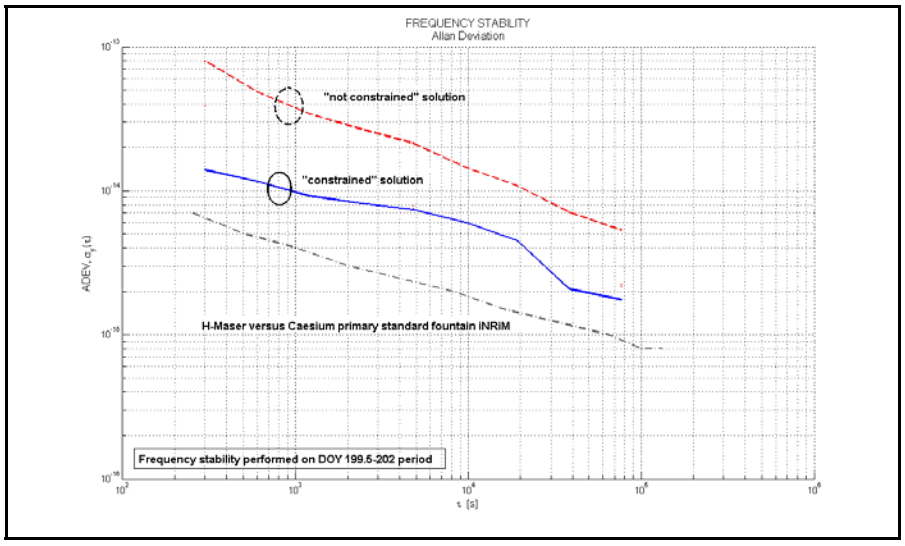

Figure 12. PPP unconstrained (red-dotted) and constrained (blue) comparison in terms of frequency stability for an intentional induced HW jump case.

NOISY RECEIVERS

In this section, the PPP constrained capabilities are evaluated in estimating clocks connected to noisy receivers. In particular, clock estimates related to another iNRiM geodetic receiver characterized to be particularly noisy are evaluated.

In Figure 13, the evaluation mentioned is carried out in terms of phase offset for both "not constrained" and "constrained" solutions, while in Figure 14 the previously mentioned analysis is carried out in terms of frequency stability.

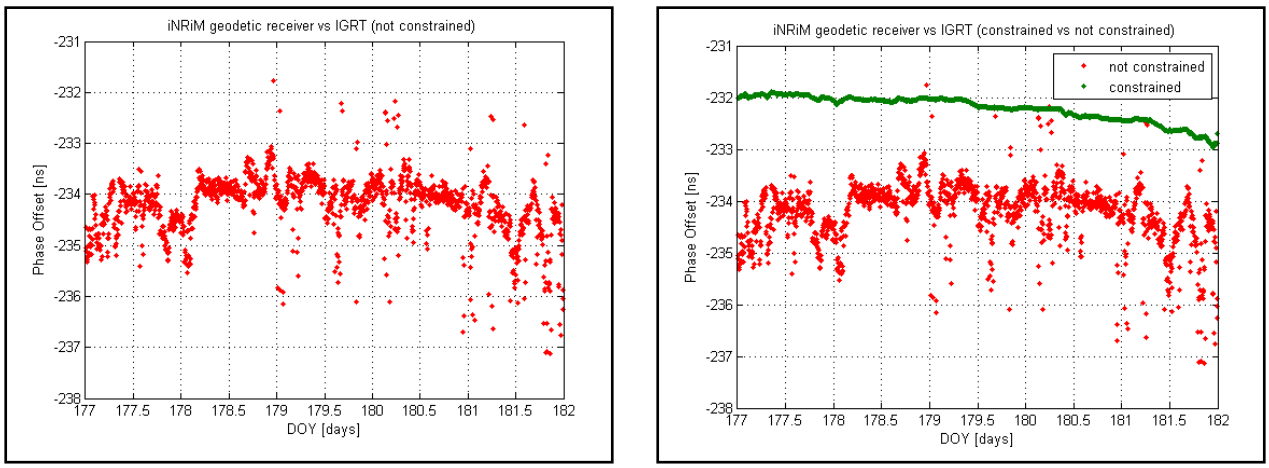

Figure 13. PPP unconstrained (red-left/right) and constrained (green-right) solutions comparison for a noisy receiver case.

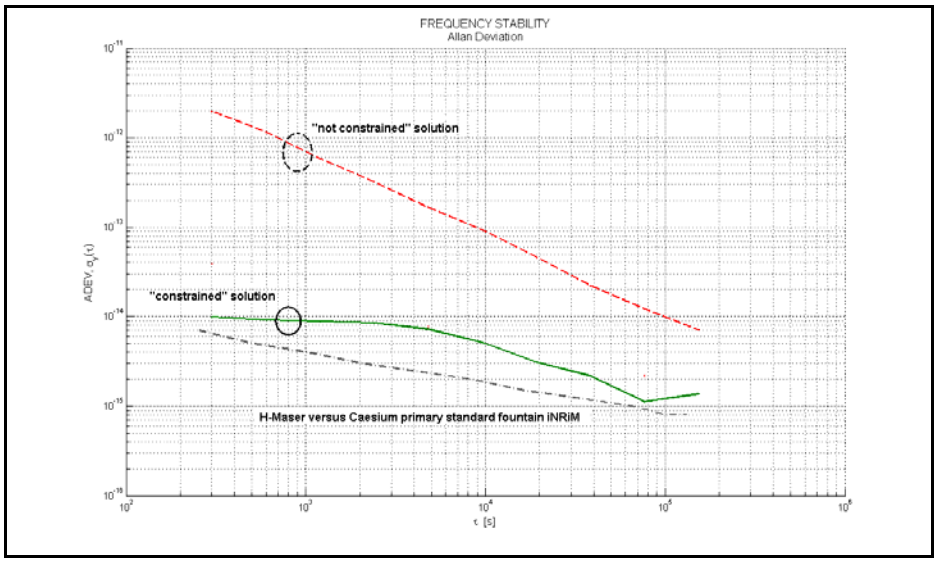

Figure 14. PPP unconstrained (red-dotted) and constrained (green) comparison in terms of frequency stability for a noisy receiver case.

As depicted in this case, not only are the short-term frequency stability performances clearly improved, but also the medium-long-term ones, after having constrained the PPP clock estimation process.

In Table II, all the deterministic and stochastic parameters taken into account for the PPP constrained solutions analyzed in the present work are listed.

Table 2. Deterministic and stochastic parameters for constrained PPP solutions.

Station (vs IGRT)	Period (DOY)	y	d	Sigma(1s)*
usn3	**120-129**	**9.1879e-15**	**1.5631e-21**	**2e-13**
usn3	**310-329**	**-9.8041e-15**	**-4.8312e-22**	**2e-13**
Ieng	**120-129**	**5.56035e-15**	**-3.4701e-21**	**2e-13**
Ieng	**310-329**	**-1.6429e-14**	**-1.1695e-21**	**2e-13**
ptbb	**120-129**	**1.7241e-15**	**8.6047e-21**	**4e-13**
opmt	**120-129**	**5.3824e-13**	**-1.5217e-20**	**2e-13**
brus	**120-129**	**1.2566e-14**	**1.9229e-20**	**2e-13**
geo1	**197-207**	**-2.5922e-13**	**-2.1464e-20**	**2e-13**
geo2	**177-181**	**-6.2695e-16**	**-4.0912e-20**	**2e-13**

*Value as spec. by the "Sigma Tau" manufacturer for an H-maser. The values used for all H-masers involved in the comparison, though, come from different manufacturers.
For the PTB Cs2 primary cesium clock, estimates are as published at 1996 IEEE International Frequency Symposium.

DISCUSSION AND CONCLUSION

In this work, preliminary evaluations about the possibility to constraint PPP clock estimation process have been carried out.

First results show that for GPS receivers driven by high-quality clocks, it is possible to reduce the short-term noise of the time transfer technique, using *a priori* clock information − noise characteristics, as well as frequency offset and linear frequency drift. This improvement is achieved without affecting "receiver clock reset" detection functionality. Values for the station clock constraint, in terms of sigma (1s) of the white frequency noise, frequency offset, and linear drift, have to be carefully estimated in order to avoid divergence and, in the next upgraded versions of PPP, they will estimated "on the fly."

Further analysis will be carried out in order to confirm preliminary results.

ACKNOWLEDGMENT

The authors wish to thank all the people in timing laboratories involved in this experiment for granting the use of their GPS data. Their contribution is highly appreciated. The authors also wish to acknowledge the many individuals and institutions forming the IGS for the high-quality GNSS products.

REFERENCES

[1] J. Ray and K. Senior, 2005, "*Geodetic techniques for time and frequency comparisons using GPS phase and code measurements,*" **Metrologia, 42**, 215-232.

[2] R. Dach, U. Hugentobler, T. Schildknecht, L.-G. Bernier, and G. Dudle, 2002, "*Precise Continuous Time and Frequency Transfer Using GPS Carrier Phase,*" 2002, **IEEE Transactions on Ultrasonics, Ferroelectrics, and Frequency Control, UFFC-49,** 1480-1490.

[3] J. Ray and K. Senior, 2003, "*IGS/BIPM pilot project: GPS carrier phase for time/frequency transfer and timescale formation,*" **Metrologia, 40,** S270-S288.

[4] K. Senior, P. Koppang, and J. Ray, 2003, "*Developing an IGS time scale,*" I**EEE Transactions on Ultrasonics, Ferrolectrics, and Frequency Control, UFFC-50,** 585-593.

[5] J. Kouba and T. Springer, 2001, "*New IGS station and satellite clock combination,*" **GPS Solutions, 4,** 31-36.

[6] J. Kouba and P. Héroux, 2001, "*Precise Point Positioning Using IGS Orbit and Clock Products*", **GPS Solutions, 5** (2), 12-28.

[7] R. Costa, D. Orgiazzi, V. Pettiti, I. Sesia, and P. Tavella, 2004, "*Performance Comparison and Stability Characterization of Timing and Geodetic GPS Receivers at IEN,*" in Proceedings of the 18th European Time and Frequency Forum (EFTF), 5-7 April, 2004, Guildford, UK.

[8] J. Ray and K. Senior, 2005, *"Geodetic techniques for time and frequency comparisons using GPS phase and code measurements,"* **Metrologia, 42,** 215-232.

[9] P. Defraigne, G. Petit, and C. Bruyninx, 2002, "*Use of geodetic receivers for TAI,*" in Proceedings of the 33rd Annual Precise Time and Time Interval (PTTI) Systems and Applications Meeting, 27-29 November 2001, Long Beach, California, USA (U.S. Naval Observatory, Washington, D.C), pp. 341-348.

[10] D. Orgiazzi, P.Tavella, and F. Lahaye, 2005, "*Experimental assessment of the Time Transfer Capability of Precise Point Positioning (PPP)*", in Proceedings of the 2005 Joint IEEE International Frequency Control Symposium and Precise Time and Time Interval (PTTI) Systems and Applications Meeting, 29-31 August 2005, Vancouver, Canada (IEEE Publication 05CH37664), pp. 337-345.

[11] P. Defraigne and C. Bruyninx, 2007, "*On the link between GPS pseudorange noise and day boundary discontinuities in geodetic time transfer solutions,*" **GPS Solutions, 11,** 239-249.

[12] N. Guyennon, G. Cerretto, P. Tavella, and F. Lahaye, "*Further Characterization of the Time Transfer Capabilities of Precise Point Positioning (PPP),*" in Proceedings of TimeNav'07, the IEEE International Frequency Control Symposium (FCS) Joint with the 21st European Frequency and Time Forum (EFTF), 29 May-1 June 2007, Geneva, Switzerland (IEEE Publication 07CH37839), pp. 399-404.

[13] R. Mannucci and F. Cordara, 1997, **Misurare il tempo e la frequenza** (Editrice Il Rostro, Milan).

[14] L. Galleani, L. Sacerdote, and P. Tavella, and C. Zucca, 2003, "*A Mathematical Model for the Atomic Clock Error,*" **Metrologia, 40,** S257-S264.

[15] D. W. Allan, 1987, "*Time and Frequency (Time-Domain) Characterization, Estimation, and Prediction of Precision Clocks and Oscillators,*" **IEEE Transactions on Ultrasonics, Ferroelectrics, and Frequency Control UFFC-34,** 647-654.